IFAC

International Federation of Automatic Control

16th IFAC Symposium on Automatic Control in Aerospace

PREPRINTS
Volume 1

Editor: Alexander Nebylov

June 14-18, 2004

CORRECTIONS OF A VESTIBULAR FUNCTION UNDER EXTREME CONDITIONS OF THE AEROSPACE FLIGHT

V. Alexandrov [*,1], S. Lemak [*], A. Shkel [**],
E. Soto [***]

* Lomonosov Moscow State University, Faculty of
Mechanics and Mathematics, Vorobjovy Gory, Moscow
119899 RUSSIA, Fax: +(095)939-28-00, E-mail:
valex@moids.math.msu.su
** Department of Mechanical and Aerospace Engeneering,
University of California, IRVINE, CA, USA, Fax:
+(949)824-85-85, E-mail: ashkel@uci.edu
*** La Universidad Autonoma de Puebla, c.p. 72570,
Mexico Tel:+(052)2229500 ext7316, E-mail:
esoto@isin.buap.mx

Abstract: Operation of the human vestibular apparatus under extreme conditions does not provide full and reliable information for personal navigation. In this connection, there is a need to correct the vestibular function. In this paper we formulate a number of problems arising in this field of research. Extreme situations are described and their dynamic simulation is considered. The structure of space simulators, based on centrifuge with three degrees of freedom (3 DOF) controlled gimbals and a special space suit with controlled air pressure, is proposed. *Copyright ©2004 IFAC*

Keywords: Centrifuge, dynamic simulation, differential game, saddle point

1. EXTREME SITUATIONS AND OPERATION OF THE VESTIBULAR SENSORY APPARATUS

The vestibular apparatus is a basic element of the animal's navigation system (in particular, of human personal navigation). Due to operation of this navigation system, an animal controls and stabilizes its movement. The vestibular apparatus (Orlov, 1998) includes 1) three semicircular canals on each lateral side of its head (these canals form two near orthogonal trihedrons) and 2) two pairs of otolithic organs (two utricles and two sacculi).

Each canal can be represented as a thin curved duct of semicircular shape filled with endolymph (a viscous incompressible fluid). Both ends of each duct are open and lowered into a reservoir (the utricle). One of these ends is sharply expanded in the immediate neighborhood of the utricle, forming an ampulla. The cupula (an elastic jellylike partition) resides inside the ampulla and is attached to the ampullary walls on the crista (a sensory base) in such a way that it is capable of deflecting in response to the motion of the endolymph. The crista contains hair sensory cells. The otolithic membrane is positioned inside the utricle. This membrane is of a complex shape, contains otoconial crystals and a jellylike mass,

and is able to displace along the macula (a sensory base of the utricle with hair sensory cells).

In order to clarify the necessity of considering extreme situations during operation of the vestibular apparatus, below we present simplified mathematical models for biomechanics of semicircular canals and otolithic organs. As a mechanotheoretical model of semicircular canal dynamics, we consider the cupula as an elastic piston inside the ampulla under endolymph pressure. The following approximate mathematical model of cupula-piston dynamics is given in (Astakhova, 1989):

$$\ddot{x}_0 + \frac{8\nu}{a^2}\dot{x}_0 + \frac{\gamma}{m_0 k^4}x_0 = -\frac{R}{k^2}\left(1 + \frac{l}{\mathcal{L}}\right)\dot{\omega}. \quad (1)$$

Here x_0 is the linear displacement of the cupula-piston relative its equilibrium position; $\dot{\omega}$ is the proection of angular acceleration (generated by rotation of the animals head) onto the axis orthogonal to the semicircular plane; R is the outer radius of the canal; a is the inner radius of the canal; a_0 is the radius of the ampulla, $k = \frac{a_0}{a_1} > 1$; $\mathcal{L}$ is the length of the canal; l is the length of the utricle, $l < \mathcal{L}$; $m_0 = \varrho\pi a^2\mathcal{L}$, where ϱ is the density of the endolymph; γ is the coefficient of elasticity of the cupula-piston; ν is the kinematic viscosity of the endolymph.

The equations describing the center-of-mass relative displacement of the otolithic membrane in the projections onto the macula axes of sensitivity Ox_1 and Ox_2 take the form

$$\frac{m_1}{m_2}\ddot{x}_1 + \frac{\nu}{m_2}\dot{x}_1 + \frac{k_2}{m_2}x_1 - (2\omega_3\dot{x}_2 + (\omega_3^2 + \omega_2^2)x_1 + (\dot{\omega}_3 - \omega_1\omega_2)x_2) = g_1 - w_1, \quad (2)$$

$$\frac{m_1}{m_2}\ddot{x}_2 + \frac{\nu}{m_2}\dot{x}_2 + \frac{k_2}{m_2}x_2 + (2\omega_3\dot{x}_1 - (\omega_3^2 + \omega_1^2)x_1 + (\dot{\omega}_3 - \omega_1\omega_2)x_1) = g_2 - w_2, \quad (3)$$

where $m_1 = (\varrho_0 + k_1\varrho)V_0$; ϱ, ϱ_0 is the density of the endolymph and otolotic membrane; V_0 is the volume of the otolithic membrane ; $k_1\varrho V_0$ is the apparent additional mass of the otolithic membrane; g_1 and g_2 are the projections of the gravitational acceleration $\mathbf{g}$; w_1 and w_2 are the projections of the absolute linear acceleration $\mathbf{w}$; ω_1, ω_2, and ω_3 are the projections of the absolute angular velocity of the animal's head.

Equations (2) and (3) model extreme situations adequately enough. Thus, we may conclude that the canal-otolithic reaction (1)–(3) of the vestibular apparatus in response to mechanical stimuli is the reaction in response to the angular acceleration $\dot{\omega}$ of the animal's head and to the apparent acceleration $(\mathbf{w} - \mathbf{g})$ of the reference point of the head. The normalized value $\mathbf{n} = \frac{1}{g_0}(\mathbf{w} - \mathbf{g})$ is called the overload (here g_0 is the gravitational acceleration at the equator). The further evolution of this reaction (mechanoelectrical transduction,

ion currents of hair cells in the crista and the macula, dynamics of neuromediator fluxes, appearance and propagation of afferent pulsations along nerve fibers) is discussed in (Sadovnichii et al., 2002). In order to describe various extreme situations arising during operation of the vestibular apparatus, we first model the beginning of the canal-otolithic reaction (1)–(3). It should be noted that the dynamics of this beginning for the reaction (1) of the semicircular canal differs from that for the reaction (2), (3) of the otolithic organ. Dynamics of the cupula-piston (see (1)) or of cupula-diaphragm corresponds to the dynamics of an overdamped torsion pendulum (Orlov, 1998). At the same time, the otolithic membrane dynamics (see (2), (3)) corresponds to that of a critically damped physical pendulum, which may give rise to eigenoscillations.

Let as consider an extreme situations in aerospace flight.

1.1 Sensorial conflicts under zero gravity.

Such an extreme situation can be observed, for example, during orbital flights. Under these conditions, the semicircular canal reaction in response to angular acceleration remains the same. However, it follows from (2) and (3) that the basic mechanical stimulus for the otolithic organ reaction is absent, since $(\mathbf{g} - \mathbf{w}) \sim 0$. Thus, the otolithic membrane dynamics under possible parametric disturbance $\omega(t)$ should be taken into account; in this case, the reactions of semicircular canals and otolithic organs become inconsistent, which causes vestibular disfunction (Kornilova et al., 1983). Many orbital experiments on fishes, amphibians, birds, and mammals were carried out in order to clarify the behavior of vestibular function in space. For example, a substantial proportion of experimental time (about 70 %) was given to such studies with biosatellites "Cosmos". The astronaut's vestibular function was studied on the orbital station "Mir" during 15 years of its operation. These experiments have provided a considerable amount of information on neuronal reactions of the vestibular apparatus in response to canal and otolithic stimulations under zero gravity and on vestibular oculomotor reactions causing an increase in delay of eye fixation (Reschke et al., 1997) (in a number of cases, this delay was responsible for emergency during visual control of spacecrafts). It should be noted that the variable delay in eye stabilization is of a chronic nature and continues after the astronaut's return to the Earth during the whole period of readaptation (Reschke et al. , 1997).

1.2 Disorientation in flight under large overloads.

Any flight with large overloads ($|\mathbf{n}(t)| > 1$) is characterized by various illusions (in particular, by appearance of false horizon and subjective vertical (Kornilova *et al.*, 1983)). Large (up to $15\,g$) and fast varying overloads cause intensive reactions of semicircular canals in response to angular acceleration, which may lead to the astronaut's disorientation and emergency in space flights. Under these extreme conditions, the vestibular apparatus operates on the verge of its capabilities and the blood supply in the vestibularoculomotor apparatus is disturbed, which may lead to temporal loss in vision and, as a consequence, to disturbances in personal navigation and manual control.

2. DYNAMIC SIMULATION OF EXTREME SITUATIONS AND CORRECTION OF VESTIBULAR FUNCTION

In order to study the vestibular function in extreme situations, early in the XXth century several special dynamic stands were developed; animals or specimens of the vestibular system were placed on these stands.

Kinematic schemes of such stands are different: rotary tables, dynamic platforms, support-type stands, centrifuges with or without gimbals, etc. In 1903, Tsiolkovsky carried out first experiments with insects in centrifuges in order to clarify their abilities to endure large overloads. In the 1920s, B. and Ch. Diringshefens and G. Stike (Glazer, 1959) initiated the formation of experimental centers to study the influence of various flight factors on humans. Gradually, centrifuges with gimbals have gained wide acceptance among different dynamic stands (Alexandrov *et al.*, 1995).

Let us consider a centrifuge with a cabin in the gimbal (Figure 1). The console of the centrifuge is capable of rotating in a horizontal plane with angular velocity $\omega_k(t)$. The gimbal is attached to the end of the console. The hemisphere of the gimbal (fork, Figure 1) has the axis of symmetry coincident with the console and is able to rotate through the command angle φ. The axis of the inner ring is fixed in its initial vertical position inside the outer ring (the boundary of the hemisphere); the inner ring is capable of rotating about this axis through the command angle ψ. The axis of the cabin (capable of rotating through the command angle γ) is fixed in the inner ring and is perpendicular to the axis of this ring. Thus, the above dynamic stand is a control mechanical system with four degrees of freedom. Let us consider the question of how to use such a stand to simulate extreme conditions.
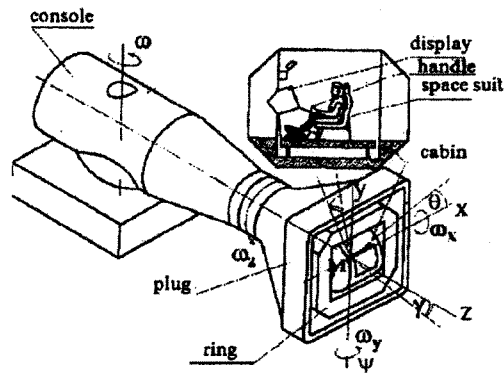

Fig. 1. A centrifuge with the controlled gimbal.

2.1 Simulation of apparent acceleration (of the overload vector $\mathbf{n}$).

Let us assume that the axis of rotation of the inner ring is initially vertical and the axis of rotation of the cabin is horizontal and is directed perpendicularly to the console. The fixed coordinate frame $O'\xi\eta\zeta$ is associated with the axis of rotation of the centrifuge (the $O'\xi$-axis is vertical). The coordinate frame $O'XYZ$ is rigidly associated with the console; the $O'X$-axis coincides with the $O'\xi$-axis and the $O'Y$-axis is directed along the console. The axes of the coordinate frame $OXYZ$ with its origin at the center of the gimbal are parallel to the axes of the coordinate frame $O'XYZ$. The coordinate frames $Ox_1y_1z_1$, $Ox_2y_2z_2$, and $Oxyz$ are rigidly associated with the fork, the inner ring, and the cabin, respectively. The transition from the coordinate frame $O'XYZ$ to the coordinate frame $Oxyz$ can be represented as follows:

$$XYZ \; \frac{\theta}{Y,\,y_1} \; x_1y_1z_1 \; \frac{\psi}{x_1,\,x_2} \; x_2y_2z_2 \; \frac{\gamma}{z_2,\,z} \; xyz.$$

Here the angles of rotation θ and ψ are introduced in a clockwise direction, whereas the angle γ is introduced in a counterclockwise direction. The overload formed by the centrifuge is equal to $\mathbf{n}^T = (n_X, n_Y, n_Z) = \left(1, \, -\dfrac{\omega^2 l}{g}, \, \dfrac{\dot{\omega} l}{g}\right)$, where n_X, n_Y, and n_Z are its projections onto the axes of the coordinate frame $OXYZ$, l is the length of the console, and ω is the rate of rotation of the console about the $O'\xi$-axis.

The projections of the overload vector $\mathbf{n}^0(t)$ onto the axes of the coordinate frame associated with the cabin are known as time functions. In the process of simulation, it is necessary to choose the angles of the gimbal and the rate of rotation of the console in such a way that the inequality $\|\mathbf{n} - \mathbf{n}^0(t)\| < \varepsilon$ be valid (here ε is an accuracy of simulation (Alexandrov, 1980)).

The algorithm for simulation of overloads can be divided into two steps. First, the required rate of rotation of the console is determined from

the solution of the problem on simulation of the overload vector magnitude. Second, the angles of rotation made by the rings of the gimbal are determined from the solution of the problem on simulation of the overload vector direction.

2.2 Training on simulation stands and corrections of vestibular function.

In Section 1 of this paper we have described the extreme situations for personal navigation when operation of the vestibular apparatus should be corrected. Two kinds of corrections for the vestibularfunction and two kinds of help for the vestibularapparatus are possible.

First, training helps a human being in faster adaptation to an extreme situation and in correction of information coming from the vestibular system (using other words, training helps in the formation of conditioned reflexes).

Second, vestibular prostheses help in the correction of vestibularfunction up to the complete replacement of this function when the vestibularapparatus does not work. Pharmacological remedies for such corrections and replacements are not discussed here.

Let us consider the first kind of corrections. It is clear that the correction training should be performed on dynamic stands; this allows one to simulate extreme situations dynamically. It was shown in this paper that the apparent acceleration (a basic mechanical stimulus for otolithic organs) can be simulated dynamically and that centrifuges with controllable gimbals are most reasonable. Generally, however, angular velocities of simulating motion may not correspond to those of actual motion. In the case of quasisteady simulating motion, according to (Alexandrov, 1980), this inconsistency is not essential. This allows us to propose an algorithm for dynamic simulation of controllable reentry from an orbit (Alexandrov et al. , 1995) and to train astronauts for the International Space Station in the Training Center named after Gagarin.

The problem of dynamic simulation can be considered in the following more complex formulation: it is required to find simulating motions such that the mechanical stimuli for the canal–otolithic system and the dynamics of canal–otolithic reactions on a stand be similar to those for actual motions.

For the above kind of corrections, another problem would require its formulation and solution. It is necessary to correct the vestibularfunction in order to refine navigational information and to improve the control of human motion or the motion of an object. Therefore, the scope and

duration of preflight training should be specified on the basis of quality testing of required experience in space control. One of the approaches to guaranteed testing is discussed in (Alexandrov, 1997),(Alexandrov et al., 1999).

3. FORMULATION OF THE PROBLEM OF TESTING

The testing procedure is based on obtaining the reliable data that characterize the stabilization accuracy for the case when the parametric and time-varying perturbations preventing the system from being stabilized are the worst possible. Such an approach was proposed in (Alexandrov, 1997), where formulations of maximin problems provide the basis for the testing strategy. In this paper, this approach is extended to the case when a statistical description is known for a certain part of perturbations, which may be represented, therefore, by steady stochastic processes with a given spectral density. As is known, such perturbations can be modeled by perturbations at the output of a linear stochastic system whose input actions may be regarded as white noise with a given intensity (Alexandrov et al., 1999) ; without loss of generality, hence, we may assume that the random perturbations acting on the system are modeled by the vector white noise with a known intensity. In this case the testing procedure leads to game problems for dispersion relations of a stochastic system (these relations are expressed in terms of deviations from the required motion of the system). Suppose the equations

$$\dot{y} = \tilde{f}(y, w, v, \xi)$$

describe the motion of a control system. Here w is the vector of control signals: $w(\cdot) \in \tilde{W} = \{w(\cdot) \in L_2^s \,|\, w(t) \in \Omega \subset R^s\}$; v is the vector of perturbations influencing the stabilization accuracy adversely: $v(t) \in V = \{v(\cdot) \in L_2^l \,|\, v(t) \in \mathcal{V} \subset R^l\}$; ξ is the vector of random perturbations modeled by a steady stochastic process. Let us consider the system of equations

$$\dot{x} = f(x, v, u, \xi) \qquad (4)$$

given in deviations $x = y - \tilde{y}$ from the desired motion $\tilde{y}(t)$ belonging to the preassigned trajectory set $Y = \{\tilde{y}(t) \in Y^0 \subset R^n, \ t_0 \le t \le t_k\}$. Here $u = w - \tilde{w}$ are the unutilized resources in control for solving the stabilization problem. Usually, the control signals are formed as functions of the time t and of the deviation estimates $\tilde{x}$: $u = u(t, \tilde{x})$. The accuracy of robust stabilization is defined by the functional class

$$J = M \left[\int_{t_0}^{t_k} (x^\top G x + u^\top N u)\, dt + x^\top(t_k) S x(t_k) \right]$$

271

where the matrices G and S are constant, symmetric, and positive semidefinite ($G^\mathsf{T} = G \geq 0$, $S^\mathsf{T} = S \geq 0$) and the matrix N is positive definite ($N^\mathsf{T} = N > 0$). It is assumed that t_0 is a fixed instant of time and t_k is the instant when the given manifold is first reached (in particular, t_k may be fixed).

The best accuracy J_0^0 (or the best result in terms of accuracy of robust stabilization) is defined as

$$J_0^0 = \sup_{v \in V} \inf_{u(\cdot) \in U} J \qquad (5)$$

The best accuracy concept coincides with that of minimax stabilization if the upper and lower bounds are attainable and a saddle point (v^0, u^0) is in existence:

$$J_0^0(u^0, v^0) = \max_{v \in V} \min_{u \in U} J(u, v) = \min_{u \in U} \max_{v \in V} J(u, v) \qquad (6)$$

The vector function v depends on the deviations and control values: $v = v(t, x, u)$. Thus, there exists a certain discrimination of control; in accordance with the Krasovskii theorem, differential game (5) has the saddle point (6) (the instant t_k is fixed). The testing procedure may be decomposed into the following three stages.

The first stage (preliminary). The best accuracy J_0^0 (a value of game (6)) and the optimal strategy $v^0(\cdot)$ of testing are determined.

The second stage (basic). The process of testing is simulated with the known strategy $v^0(\cdot)$.

The third stage (final). Two comparisons are performed:

a) the best accuracy J_0^0 with the point and (or) interval estimates of the functional $J(u^r, v^0)$ obtained in accordance with the results of simulation:

b) the stabilization strategy $u^r(\cdot)$ with the best control $u^0(\cdot)$ obtained at the first stage.

4. CORRECTION OF VESTIBULAR FUNCTION BY MICRO-ELECTRO-MECHANICAL SYSTEMS

The principle use of gyroscopes is to measure orientation, heading, or pointing direction. By now, many different gyroscope concepts have been developed: from high-end inertial navigation instruments to low-end consumer product sensors (Shkel, 2001). This diversity in performance and operational requirements has spawned a vast diversity in gyroscope technology: for example, spinning wheel, vibrating tuning fork, solid-state laser, and magnetohydrodynamic gyroscopes. Almost all the high-end precision technologies are characterized by high cost, large sizes, and appreciable power consumption; at the same time, the use of

micromachining technology allows one to design inexpensive miniature gyroscopes with good performance.

Mechanical microgyroscopes are emerging from the technology developed for integrated circuits (IC). The recent advance in computer processor technology has led to a considerable demand for small systems or Micro-Electro-Mechanical Systems (MEMS) that can fully exploit the benefits of IC microtechnology. The IC industry's ability to deposit and etch micron-scale features in silicon and aluminum has been exploited to build tiny inertial sensors. The compatibility of MEMS and IC allows the integration of mechanical structures alongside microcircuits on one and the same chip. These studies are successfully conducting at California University, USA (Shkel, 2002).

Placing interface electronics, signal processing circuits, and analog-to-digital conversion on a chip results in improved noise performance, extreme miniaturization, and inexpensive manufacturing. The need for a multitude of discrete components on large printed circuit boards is virtually eliminated. Potentially, a device that is able to accurately sense, extract, and transmit three dimensional motion can be built on a single silicon chip and fit in a volume smaller than one cubic centimeter.

A prototype of the semicircular canal prosthesis was designed due to the MEMS-based technology. The purpose of such a prosthesis is to restore balance function. Ideally, the prosthesis will be able to sense motion with sufficient precision and to deliver signals to the central neural system matching signals that the natural organ would generate.

The classical micromachined gyroscope is composed of a spinning wheel or rotor which exhibits Coriolis acceleration when an object rotates due to conservation of angular momentum. Unfortunately, the scaling laws do not allow to fabricate microgyroscopes operating on rotational principle (due to unfavorable scaling of friction and significant decrease in mass). In recent years, several new approaches were proposed to design and build gyroscopes which are microscopic in size and are able to sense angular rotation using vibrational elements (Shkel, 2002).

In the vibratory gyroscopes based on this principle, the structure is driven into resonance and the rotation-induced Coriolis force causes the transfer of energy from the driven vibrational mode to a sense vibrational mode. The magnitude of energy transferred is proportional to the rate of rotation. An ensemble of six inertial MEMS sensors integrated on a single silicon chip is required to measure six-degrees of freedom of the head motion.

Our first prototype of the vestibular prosthesis is implemented using polysilicon surface micromachining technology. In the prosthesis, the three semicircular canals are replaced by three-axes MEMS gyroscopes, while the two otolith organs are replaced by three-axes accelerometers. The MEMS accelerometer consists of a proof mass suspended by compliant beams anchored to a fixed frame.

External acceleration (due to motion of the object to which the sensor's frame is attached) displaces the support frame relative to the proof mass, which in turn, changes the initial stress in the suspension spring. Both this relative displacement and the suspension-beam stress can be used as a measure of the external (apparent) acceleration.

Our micromachined gyroscopes use a vibrating element to measure the rotational velocity on the basis of the Coriolis principle.

The above-described principle of operation is not the only option for implementation of MEMS gyroscopes. Multidegree-of-freedom gyroscopes and vibratory gyroscopes capable of measuring the angle of rotation directly are also proposed (Shkel, 2001).

Thus, the sensing unit of the proposed vestibular prosthesis should include three-axes accelerometers and three-axes gyroscopes implemented on the same silicon chip. Technologically, this goal can be achieved. The above-described configuration of microdevices allows us to measure all six-degrees-of-freedom motions of the human head. The output signals from the accelerometers and gyroscopes are voltages proportional to linear accelerations and angular velocities, respectively. The rotational perceptual threshold in humans was determined to be between 0.1 and 2 grad/s^2. It should be noted, however, that perceptual thresholds are different for different rates of acceleration and vary from person to person. Montandon determined that the threshold is 1 grad/s^2 in healthy individuals, but greater than $6-7$ grad/s^2 in patients with vestibular disfunction. The reported sensation limits set the sensitivity requirements for the vestibular prosthesis. Our results and results of other groups working on MEMS inertial sensors demonstrated that the required performance level is readily achievable (Shkel, 2001).

The gyroscope is able to sense any type of angular rotation (constant or nonconstant angular velocities), while the natural vestibular organ is only responding to the angular acceleration. In order to mimic the natural organ, therefore, the supporting circuit electronically differentiates the output voltage from the gyroscope to produce a signal proportional to the angular acceleration. In our prototype, the circuit uses a low-pass filter before the differentiator for minimizing the effect of high-frequency noise (Liu et al., 2003).

REFERENCES

Orlov, I.V. (1998). *Vestibular Function* St. Petersburg.(in Russian)

Astakhova, T.G. (1989). A mathematical model for a semicircular canal of the vestibular system as an angular acceleration sensor. *Vestn. Mosk. Univ. Matem. Mekhan.*, 1, pp. 69–72.

Sadovnichii,V.A. V.V. Alexandrov, T.B. Alexandrova, A. Almanza, T.G. Astakhova, R. Vega, N.V. Kulikovskaya, E. Soto, and N.E. Shulenina (2002). A mathematical model for the mechanoreceptor of angular accelerations. *Vestn. Mosk. Univ. Matem. Mekhan.*, 6 pp. 46–55.

Kornilova,L. L. Jakovleva, N. Tarasov, and G. Gorgiladze (1983). Cosmonaut's vestibular disfunction during microgravitation adaptation and readaptation. *Physiologist*, 20, pp. 535–536.

Reschke,M. L. Kornilova, D. Harm, et. al. Neurosensory and sensory-motor function. *Space Biology and Medicine, Joint US/Russian Publication. AIAA* 3, 1, pp. 135–193.

Alexandrov, V.V. L.I. Voronin, Yu.N. Glazkov, A.Yu. Ishlinsky, and V.A. Sadovnichii (1995). *Mathematical Problems of Dynamic Simulation in Space Flights* Moscow.(in Russian)

Glaser,G. (1959). *Dramatische Medizin* (in German), Zürich.

Alexandrov,V.V. (1980). Simulation of apparent accelerations. *Dokl. Akad. Nauk SSSR* **256**, 2, pp.345–348.

Alexandrov,V.V. (1997). Quality testing in stabilization of unsteady motions. *Vestn. Mosk. Univ. Matem. Mekhan.*, 3, pp. 51–54.

Alexandrov,V.V. S.S. Lemak, and D. Vera Mendoza (1999). Accuracy testing in magnetic stabilization of small satellites. *Vestn. Mosk. Univ. Matem. Mekhan.*, 5 pp. 66–73.

Shkel,A. (2001). Micromachined gyroscopes: challenges, design solutions, and opportunities. *The 2001 SPIE Annual International Symposium on Smart Structures and Materials (Invited Paper)*, Newport Beach.

Shkel,A. and R.T. Howe (2002). *Micromachined Angle-Measuring Gyroscope*, U.S. Patent 6,481,285, Nov. 19, 2002.

Liu,J. A. Shkel, K. Nie, and F. Zeng (2003). System design and experimental evaluation of a mems-based semicircular canal prosthesis. *Proc. Int. IEEE EMBS Conf. on Neural Engineering*, Capri Island.